

THE VARIED FATES OF $z \sim 2$ STAR-FORMING GALAXIES

CHARLIE CONROY¹, ALICE E. SHAPLEY^{1,2,3}, JEREMY L. TINKER⁴, MICHAEL R. SANTOS^{5,6}, GERARD LEMSON^{7,8}

Draft version October 31, 2018

ABSTRACT

Star-forming galaxies constitute the majority of galaxies with stellar masses $\gtrsim 10^{10} h^{-2} M_{\odot}$ at $z \sim 2$. It is thus critical to understand their origins, evolution, and connection to the underlying dark matter distribution. To this end, we identify the dark matter halos (including subhalos) that are likely to contain star-forming galaxies at $z \sim 2$ (z2SFGs) within a large dissipationless cosmological simulation and then use halo merger histories to follow the evolution of z2SFG descendants to $z \sim 1$ and $z \sim 0$. The evolved halos at these epochs are then confronted with an array of observational data in order to uncover the likely descendants of z2SFGs. Though the evolved halos have clustering strengths comparable to red galaxies at $z \sim 1$ and $z \sim 0$, we find that the bulk of z2SFGs *do not* evolve into red galaxies, at either epoch. This conclusion is based primarily on the fact that the space density of z2SFGs is much higher than that of lower redshift red galaxies, even when accounting for the merging of z2SFG descendants, which decreases the number density of z2SFG descendants by at most a factor of two by $z \sim 0$. Of the $\sim 50\%$ of z2SFGs that survive to $z \sim 0$, $\sim 70\%$ reside at the center of $z \sim 0$ dark matter halos with $M > 10^{12} h^{-1} M_{\odot}$. Halo occupation modeling of $z \sim 0$ galaxies suggests that such halos are occupied by galaxies with $M_r \lesssim -20.5$, implying that these z2SFGs evolve into “typical” $\sim L^*$ galaxies today, including our own Galaxy. The remaining $\sim 30\%$ become satellite galaxies by $z \sim 0$, and comparison to halo occupation modeling suggests that they are rather faint, with $M_r \lesssim -19.5$. These conclusions are at least a partial departure from previous work due primarily to the increased accuracy of observational data at $z \lesssim 1$, and to higher resolution N -body simulations that explicitly follow the evolution of dark matter subhalos, whose observational counterparts are likely satellite galaxies. These conclusions are qualitatively generic in the sense that any halo mass-selected sample of galaxies at one epoch will evolve into a more complex and heterogeneous sample of galaxies at a later epoch. This heterogeneity is driven largely by the fact that some galaxies will continue to accrete matter and form stars throughout their evolution, while others will become satellites and thus have their growth suppressed relative to galaxies in the field.

Subject headings: galaxies: evolution — galaxies: halos — galaxies: high-redshift

1. INTRODUCTION

The past decade has witnessed an enormous increase in our knowledge of the high-redshift ($z > 2$) Universe. The unique rest-frame UV spectral signatures of star-forming galaxies have allowed observers to select galaxies at $z \gtrsim 2$ based solely on optical photometry with very high efficiency (e.g. Steidel et al. 2003, 2004). Extensive multi-wavelength follow-up of these objects, including optical and near-IR spectroscopy, and imaging at wavelengths from X-ray through radio, has yielded estimates of rest-frame UV luminosities and colors (Steidel et al. 1999; Adelberger & Steidel 2000; Reddy et al. 2007), stellar masses (Shapley et al. 2005; Erb et al. 2006c), star-formation rates (Erb et al. 2006b; Reddy et al. 2006), chemical abundances (Pettini et al. 2001; Erb et al. 2006a), and clustering strengths (Adelberger et al. 2003, 2005; Giavalisco & Dickinson 2001; Ouchi et al. 2005; Lee et al. 2006; Hamana et al. 2006; Quadri et al. 2007) of a

large, well-defined population of galaxies that dominate the star-formation rate density (Reddy et al. 2007) at an epoch when the Universe was only a few billion years old. Complementary techniques tuned to the rest-frame optical properties of galaxies at similar epochs have identified objects with typically redder colors and higher mass-to-light (M/L) ratios, but the corresponding spectroscopic confirmation has only been obtained for the brightest, rare objects (Franx et al. 2003; Daddi et al. 2004; van Dokkum 2006).

At the same time, models connecting galaxies to the underlying dark matter distribution have been put forth which either focus on quantifying the statistical relation between galaxies and dark matter halos (e.g. Berlind & Weinberg 2002; Bullock et al. 2002; Yan et al. 2003; Seljak 2000; Scoccimarro et al. 2001; Zheng 2004; Kravtsov et al. 2004; Conroy et al. 2006), or predicting the connection based on physical principles (e.g. White & Frenk 1991; Somerville & Primack 1999; Cole et al. 2000; Hattton et al. 2003; Springel et al. 2001a; Croton et al. 2006; Bower et al. 2006). Essential to these latter efforts has been the vast increase in size and resolution of N -body simulations, which has only recently allowed for the construction of detailed merger trees that follow not only the evolution of distinct halos, i.e. those halos not contained within any larger halo, but also subhalos — the halos contained within the virial radii of distinct halos — whose observational counterparts are likely satellite galaxies (e.g. Springel et al. 2001a). Throughout we refer to both distinct halos and subhalos generically as halos. Despite impressive advances in our understanding both of the

¹ Department of Astrophysical Sciences, Princeton University, Princeton, NJ 08544

² Alfred P. Sloan Fellow

³ David and Lucile Packard Fellow

⁴ Kavli Institute of Cosmological Physics, University of Chicago, Chicago, IL 60637

⁵ Space Telescope Science Institute, 3700 San Martin Dr., Baltimore, MD 21218

⁶ Giacconi Fellow

⁷ Astronomisches Rechen-Institut, Zentrum für Astronomie der Universität Heidelberg, Moenchhofstr. 12-14, 69120 Heidelberg, Germany

⁸ Max-Planck Institut für extraterrestrische Physik, Giessenbach Str., 85748 Garching, Germany

properties of halos themselves and of the relation between galaxies and halos, fundamental questions remain.

The origin and fate of z2SFGs is one such question. Herein we define z2SFGs as those galaxies selected to lie at $z \sim 2$ based on optical U_nGR photometry that are brighter than $R = 25.5$, which corresponds to a rest-frame UV magnitude limit at this epoch. Historically, UV-selected high-redshift galaxies have been described as either low-mass, merger-induced starbursts or more massive galaxies “quiescently” forming stars. With early data, it was not possible to distinguish between these opposing ideas (Lowenthal et al. 1997; Coles et al. 1998; Mo et al. 1999; Giavalisco & Dickinson 2001; Kolatt et al. 1999; Somerville et al. 2001; Wechsler et al. 2001). However, recent modeling in conjunction with more recent data on the abundance and spatial clustering seems to favor the latter picture (Conroy et al. 2006; Adelberger et al. 2005). The distribution of stellar populations of these objects lends support to the massive, quiescent scenario as well (Shapley et al. 2001; Erb et al. 2006c).

Once identified at high redshift, it is also important to determine what type(s) of galaxies z2SFGs evolve into at later epochs. Most previous analyses have focused on the so-called Lyman-Break Galaxies, which are UV-selected star-forming galaxies at $z \sim 3$. We argue in later sections that these galaxies are qualitatively similar to z2SFGs and thus here we make no distinction between the two. Some analyses focusing on the strong observed clustering of z2SFGs favored the scenario where z2SFGs evolved into the observed massive red galaxies at $z \sim 1$, and by $z \sim 0$ were at the centers of rich groups and clusters (Mo & Fukugita 1996; Baugh et al. 1998; Governato et al. 1998, 2001; Blaizot et al. 2004; Adelberger et al. 2005), though other models incorporating the high observed comoving number density of z2SFGs suggested a more nuanced history (Moustakas & Somerville 2002). Subsequent to these efforts, there has been a vast increase in our understanding of the number densities and clustering of galaxies as a function of luminosity and color both at $z \sim 1$ (e.g. Coil et al. 2006; Pollo et al. 2006; Meneux et al. 2006; Coil et al. 2007) and $z \sim 0$ (e.g. Zehavi et al. 2005). Better constraints on the statistics of galaxy populations at lower redshift are crucial for a robust identification of the descendants of high-redshift galaxies. These recent data at $z \leq 1$, in conjunction with new high-resolution simulations and dark-matter-halo merger trees, motivate a re-evaluation of the nature and subsequent evolution of z2SFGs.

In the present work we focus on the fate(s) of observed z2SFGs. This redshift range is our focus here rather than $z \geq 3$, as there has been much recent attention to this lower redshift window with several complementary galaxy selection techniques. Plus, a more extensive set of multi-wavelength imaging and spectroscopy exists for $z \sim 2$ galaxies, allowing the more robust estimate of a number of physical properties such as stellar, gas, and dynamical masses, and extinction-corrected star-formation rates (Erb et al. 2006c; Shapley et al. 2005; Förster Schreiber et al. 2006; Reddy et al. 2006), which are important to consider along with the inferred host dark-matter halo properties. Such a detailed comparison of halo and galaxy masses and formation histories is currently not possible at higher redshifts.

Under the assumption of a tight correlation between galaxy light and halo mass, the observed clustering of z2SFGs puts a constraint on the minimum halo mass hosting such galaxies (§2). Halo merger trees extracted from a cosmological

N -body simulation are then used to follow the halos hosting z2SFGs to later epochs. Comparing the clustering, satellite fraction, and number density of these evolved halos to observed galaxy populations at both $z \sim 1$ and $z \sim 0$ then provides constraints on the fates of z2SFGs (§3).

Throughout we assume a Λ CDM cosmology with $(\Omega_m, \Omega_\Lambda, \sigma_8) = (0.25, 0.75, 0.9)$, consistent with the *WMAP* data (Spergel et al. 2003). Where applicable, we leave results in terms of h , the Hubble parameter in units of $100 \text{ km s}^{-1} \text{ Mpc}^{-1}$. In several sections we discuss how our results are affected by adopting the cosmological parameters favored by the *WMAP3* data (Spergel et al. 2007), where the primary difference is a lower σ_8 . Halo masses are measured as the mass interior to a region with mean enclosed density equal to 200 times the critical density. A Chabrier (2003) IMF is assumed when quoting stellar masses. All magnitudes are quoted in the AB system; we omit the factor of $5 \log(h)$ when quoting absolute magnitudes for brevity.

2. PRELIMINARIES

2.1. Connecting Galaxies to Halos

The clustering strength of a given sample of galaxies can be used to estimate the minimum dark matter halo mass, M_{\min} , hosting such galaxies, for a specified Λ CDM cosmology (see e.g. Wechsler et al. 1998, 2001; Adelberger et al. 2003; Quadri et al. 2007; Gawiser et al. 2007). This approach assumes that a sample of galaxies above a given luminosity threshold corresponds, at least approximately, to a sample of halos above a given mass threshold. Under this assumption, the threshold M_{\min} is varied until the clustering of halos with $M \geq M_{\min}$ matches that of the observational sample in question.

While early attempts only considered distinct halos, recent work has demonstrated that this approach can be refined by including dark matter subhalos — halos that orbit within the potential wells of distinct halos — as possible sites for galaxies (e.g. Colín et al. 1999; Kravtsov & Klypin 1999; Springel et al. 2001a; Kravtsov et al. 2004; Tasitsiomi et al. 2004; Vale & Ostriker 2004, 2006; Conroy et al. 2006). The approach is as simple as before — M_{\min} is varied until a match with the observed correlation function is obtained — except now galaxies can reside within subhalos, and hence there can be multiple galaxies per distinct halo. This refinement is desirable because the observed correlation function requires there to be multiple galaxies per distinct halo (e.g. Zehavi et al. 2005).

In this model, the space density of halos with $M \geq M_{\min}$ need not match the space density of observed galaxies. This approach thus allows the possibility of there being fewer than one galaxy per halo or subhalo, which, if favored by the data, would indicate that z2SFGs are “on” only a fraction of the time (Martini & Weinberg 2001). Such a scenario may arise if the star-formation in these galaxies is episodic due to, for example, major mergers. The converse possibility, where there is more than one galaxy per halo, would signal an inconsistency in the model, since the model assumes that halos (both distinct and subhalos) can host at most one galaxy.

Previous work has demonstrated that better agreement with observed small-scale clustering data can be achieved when using the subhalo mass at the time when it is accreted on to a larger halo (at the “epoch of accretion”), rather than its present day mass (Nagai & Kravtsov 2005; Vale & Ostriker 2006; Conroy et al. 2006; Wang et al. 2006; Berrier et al. 2006).

The accretion epoch mass is expected to correlate more strongly with galaxy properties because, while a subhalo can experience mass-loss due to tidal stripping, the galaxy, which is embedded at the very center of the halo, is much less affected by tidal evolution. For subhalos, we use this accretion-epoch mass herein when counting halos above M_{\min} , but note that the dynamical times at $z \sim 2$ are short (~ 0.1 Gyr) and thus subhalos merge rapidly. Therefore, those that are identified at $z \sim 2$ were only accreted rather recently. In fact, more than half of the subhalos identified in the simulation at $z \sim 2$ above our best-fit M_{\min} (see below) were accreted within the last simulation output, which at these epochs is ~ 0.2 Gyr. Because of their recent accretion, they have thus lost little mass due to the effects of tidal stripping; the average halo has lost 30% of its mass since accretion, as inferred from a high-resolution N -body simulation (see below). The difference between using accretion-epoch versus current masses should thus be small; we include it only for completeness.

In sum, we vary M_{\min} until the clustering of the halos with $M \geq M_{\min}$ matches the clustering of the observed z2SFGs. We include both distinct halos and subhalos so that there can be multiple galaxies per distinct halo (as there are multiple galaxies per group/cluster). For subhalos we use the subhalo mass at the epoch of accretion as this should be a better proxy for the stellar, and hence luminous, content of the subhalo.

As applied to z2SFGs, the approach outlined above assumes that the rest-frame UV luminosity of galaxies is tightly and monotonically correlated with dark matter halo mass. Since this does not appear to be the case at $z \sim 0$ (e.g. Heinis et al. 2007), such an assumption may at first glance appear unjustified. In fact, however, several lines of evidence suggest that this assumption is valid at $z \sim 2$. The most straightforward evidence comes from the fact that the large scale clustering strength of observed z2SFGs is an increasing function of rest-frame UV luminosity (Adelberger et al. 2005) at the $\sim 2\sigma$ level. Larger samples at somewhat higher redshifts ($3 < z < 5$) confirm this trend (Ouchi et al. 2005; Lee et al. 2006). Such facts are most readily understood if there is a correlation between UV luminosity and halo mass since higher mass halos are more strongly clustered than lower mass halos. At lower redshift, this general line of reasoning is routinely employed (e.g. Zehavi et al. 2005; Conroy et al. 2006), and has been verified by more direct measurements of halo mass, such as weak gravitational lensing (e.g. Mandelbaum et al. 2006).

Further evidence comes from the observation of a clear correlation between the star-formation rate and baryonic mass (stellar mass and cold gas mass within ~ 6 kpc) for z2SFGs (Erb et al. 2006b,c). If the vast majority of galaxies at $z \sim 2$ are forming stars vigorously enough to be detected as z2SFGs, as appears to be the case (Franx et al. 2003; Daddi et al. 2004; van Dokkum 2006), then a selection on rest-frame UV luminosity, which traces star-formation – modulo the effects of dust extinction – should correspond to a selection on baryonic mass. Since a strong redshift-independent correlation between baryonic and halo mass is a firm prediction of any theory of galaxy formation (e.g. Crain et al. 2007), a UV luminosity-limited sample is approximately a halo mass-selected sample at these epochs.

There is thus ample evidence that rest-frame UV luminosity is tightly correlated with halo mass at $z \sim 2$. However, the lack of any strong dependence of clustering on UV luminosity at $z \sim 0$ suggests that this is not the case in the local Universe (e.g. Heinis et al. 2007). We now briefly provide a plausible

explanation for this difference between high and low redshift.

At high redshift, star-formation and baryonic mass are monotonically related primarily because most of the gas in halos at high redshift is cold ($\sim 10^4$ K), and so it directly contributes to the star-formation rate (e.g. Kereš et al. 2005). Only galaxies within the most massive and hence rarest halos have had star-formation largely truncated at this epoch (Franx et al. 2003; Daddi et al. 2004; van Dokkum 2006; Quadri et al. 2007). At later times, infalling gas in massive halos is shock-heated to the virial temperature of the halo ($\sim 10^7$ K; White & Rees 1978; Kereš et al. 2005; Dekel & Birnboim 2006; Cattaneo et al. 2007). High temperature gas is much more susceptible to further heating processes, and thus we can assume that once gas is shock-heated, it remains hot forever (observations indicate that this must be the case for the hot gas that permeates groups and clusters of galaxies; Peterson et al. 2003). The transition from predominantly low- to high-temperature gas quenches star-formation in high mass halos, thereby breaking the monotonic relation between star formation and baryonic (and thus halo) mass. These trends are generically reproduced in hydrodynamic cosmological simulations (e.g. Blanton et al. 2000; Kereš et al. 2005; Cattaneo et al. 2007), and provide a justification of our assumption that UV light and halo mass are tightly correlated at high redshift, despite the absence of such a trend at lower redshift.

2.2. Data at $z \sim 2$

The observed z2SFGs are selected by U_nGR color cuts and required to be brighter than $\mathcal{R} = 25.5$. These are objects satisfying the “BX/MD” criteria of Steidel et al. (2004, 2003), but their comoving number density has been corrected for the incompleteness arising from star-forming galaxies scattering out of the U_nGR color selection region due to photometric errors (see e.g. Adelberger et al. 2004, 2005; Reddy et al. 2007). This sample is thus meant to encompass all star-forming galaxies at $z \sim 2$ with $\mathcal{R} \leq 25.5$. As estimated from the rest-frame UV luminosity function, the number density of these galaxies is $11 \times 10^{-3} h^3 \text{ Mpc}^{-3}$, with an uncertainty of $\sim 10\%$ (Reddy et al. 2007). This is $\sim 80\%$ higher than the preliminary number density estimates reported in Adelberger et al. (2005).

The photometric limit in the observed \mathcal{R} -band corresponds to the rest-frame UV at these epochs. At $z \sim 2$ $M^*(1700\text{\AA}) = -20.2$ and $\mathcal{R} = 25.5$ corresponds to $M^*(1700\text{\AA}) = -18.6$; the z2SFG sample thus extends ~ 1.6 magnitudes below M^* (Reddy et al. 2007). This rest-frame UV limit approximately corresponds to an unobscured star-formation rate threshold of $15 M_{\odot} \text{ yr}^{-1}$, given the typical z2SFG rest-frame UV extinction factors of $\sim 4-5$ (Steidel et al. 2004; Reddy et al. 2007).

The angular clustering of these z2SFGs has been measured by Adelberger et al. (2005), who find that the observed clustering can be fit with a real-space (de-projected) correlation function that is a power-law, $\xi = (r/r_0)^{-\gamma}$, with $\gamma = 1.6 \pm 0.1$ and $r_0 = 4.2 \pm 0.5 h^{-1} \text{ Mpc}^9$. Note that while the number density has been completeness corrected, the clustering measurements have not. That is, Adelberger et al. (2005) only mea-

⁹ The de-projection of the observed angular correlation function that yields estimates of r_0 and γ is cosmology-dependent. The results reported by Adelberger et al. (2005) assumed a cosmology where $(\Omega_m, \Omega_{\Lambda}, \sigma_8) = (0.30, 0.70, 0.9)$ — slightly different from the one adopted herein. We expect that the change in r_0 induced by updating the cosmology is within 1σ of the value reported above.

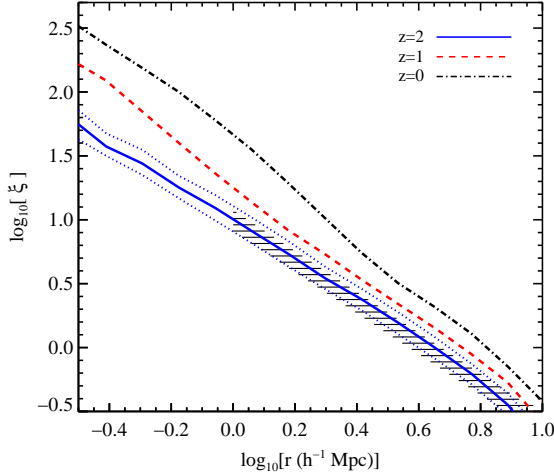


FIG. 1.— The correlation function for halos with $M \geq 10^{11.4} h^{-1} M_{\odot}$ at $z \sim 2$ (solid line) that have clustering properties similar to observed z2SFGs (hatched region; Adelberger et al. 2005). Also plotted are the correlation functions of those halos evolved to $z \sim 1$ and $z \sim 0$. The correlation function increases toward lower redshift both because of the increased clustering of halos and because of the higher satellite fraction at later times, which increases the weight given to higher mass (more clustered) halos. Halos with masses $M \geq 10^{11.2} h^{-1} M_{\odot}$ and $M \geq 10^{11.6} h^{-1} M_{\odot}$ at $z \sim 2$ are included for comparison (lower and upper dotted lines, respectively).

sured the correlation function for objects satisfying the $U_n GR$ color criteria. We are thus assuming that the objects not included in the clustering analysis have the same clustering properties as those that were included. Since $\mathcal{R} \leq 25.5$ star-forming galaxies were missed from the color selection due primarily to photometric scatter (i.e. by random processes), this assumption is well motivated (Reddy et al. 2007).

2.3. N-Body Simulations

The properties and histories of dark matter halos are taken from the Millennium simulation, a large cosmological N -body simulation with sufficient resolution to identify both distinct halos and subhalos (Springel et al. 2005). Here and throughout distinct halos are those halos that are not contained within any larger virialized system while subhalos are halos whose centers are contained within the virial radii of larger systems. This classification is analogous to the distinction between central and satellite galaxies. The simulation box has length $500 h^{-1}$ Mpc, particle mass $m_p = 8.6 \times 10^8 h^{-1} M_{\odot}$, and was run with the following cosmological parameters: $\sigma_8 = 0.9$, $\Omega_m = 1 - \Omega_{\Lambda} = 0.25$, $h = 0.73$, and $n_s = 1$ where n_s is the slope of the initial linear power spectrum. Halo merger trees, which connect halos across time, also exist for this simulation¹⁰ (Springel et al. 2005), and are utilized below. In particular, the merger trees are used to define the accretion-epoch mass for subhalos as the mass when the subhalo was last considered a distinct halo. Working with a simulation of this size can be computationally expensive; for this reason we thus make use of a $150^3 h^{-3} \text{ Mpc}^3$ region of the simulation. This size is sufficient for our purposes; for example, making use of a $250^3 h^{-3} \text{ Mpc}^3$ region at $z \sim 2$ has a negligible effect on our conclusions at that epoch.

In order to investigate the sensitivity of our results to cosmological parameters, we performed two additional N -body simulations. One used the same cosmological parameters as the Millennium run, and the other used cosmological parameters from the WMAP3 results ($\Omega_m = 0.239$, $\Omega_{\Lambda} = 0.761$, $\Omega_b = 0.04166$, $h = 0.73$, $n_s = 0.953$, $\sigma_8 = 0.756$; Spergel et al. 2007). Each simulation contained 512^3 particles in a box of length $141.3 h^{-1}$ Mpc, resulting in a particle mass of $1.46 \times 10^9 h^{-1} M_{\odot}$ for the Millennium cosmology and $1.39 \times 10^9 h^{-1} M_{\odot}$ for the WMAP3 cosmology. The GADGET-2 N -body code (Springel et al. 2001b, 2005) with a Plummer-equivalent softening length of $7.9 h^{-1} \text{ kpc}$ was used for both simulations.

In these additional simulations, we identified distinct halos with a friends-of-friends algorithm¹¹ using a linking length of 0.2 in units of the mean interparticle separation. The halos of interest contained at least 70 particles. No subhalo detection was performed on these simulations. We define halo mass as the mass within a sphere centered on the minimum potential energy halo particle (after removing unbound particles) and enclosing a density equal to 200 times the critical density. This definition closely matches the definition of $M_{\text{crit},200}$ used in the Millennium simulation (which first removed subhalo particles before identifying the halo particle with minimum potential energy) and elsewhere in this paper.

The descendant of a $z \sim 2$ halo was identified by finding the halo at a later time that contained the plurality of the particles comprising the $z \sim 2$ halo. However, the position of the descendant was taken to be the later-time center-of-mass of the particles comprising the $z \sim 2$ halo. We explicitly verified that our simulation with the Millennium cosmology produced consistent distinct halo mass functions, clustering as a function of halo mass, and halo descendant clustering as a function of halo mass as the Millennium simulation.

3. RESULTS

3.1. The z2SFG-Halo Connection

The clustering of halos extracted from the simulation at $z \sim 2$ is shown in Figure 1 for our best-fit M_{min} threshold, along with the observed z2SFG clustering. As discussed in §2.3, here and throughout “halos” refers to both distinct halos and subhalos. The clustering of halos with $M_{\text{min}} \pm 0.2$ dex from the best-fit M_{min} is included for comparison. It is clear from the figure that $M_{\text{min}} = 10^{11.4} h^{-1} M_{\odot}$ provides a good match to the observed clustering of z2SFGs. The slope of the halo correlation function on scales $1 < r < 10 h^{-1} \text{ Mpc}$ is -1.5 which is consistent at the 1σ level with the slope inferred from observations (-1.6). This figure also contains the clustering of the $z \sim 2$ halos evolved to $z \sim 1$ and $z \sim 0$, based on the Millennium simulation merger trees. The space density of $z \sim 2$ halos with $M \geq M_{\text{min}}$ is $7.5 \times 10^{-3} h^3 \text{ Mpc}^{-3}$.

The uncertainties of the z2SFG clustering data translates into an uncertainty on M_{min} of $\sim \pm 0.2$ dex (as determined by eye; see Figure 1). This uncertainty affects both the inferred number densities and the clustering strength of the corresponding host halos. For $M_{\text{min}} = 10^{11.2} h^{-1} M_{\odot}$ the number density is $13 \times 10^{-3} h^3 \text{ Mpc}^{-3}$ while for $M_{\text{min}} = 10^{11.6} h^{-1} M_{\odot}$ it is $4.3 \times 10^{-3} h^3 \text{ Mpc}^{-3}$. This range brackets the observed number density of z2SFGs ($11 \times 10^{-3} h^3 \text{ Mpc}^{-3}$) and indicates

¹⁰ The merger trees and halo catalogs are publically available and can be found here: <http://www.mpa-garching.mpg.de/millennium>.

¹¹ The algorithm we use has been made freely available by the University of Washington HPCC group: <http://www-hpcc.astro.washington.edu/tools/fof.html>.

that, within the uncertainty, every halo above M_{\min} contains one z2SFG. The uncertainty in M_{\min} is explicitly incorporated into our uncertainty in the clustering of z2SFG halos and their descendants in the following sections.

In reality the dark matter halo occupation function of z2SFGs need not be a step function at M_{\min} (zero galaxies per halo/subhalo below M_{\min} and one above it). For example, scatter between galaxy UV luminosity and halo mass at $z \sim 2$ will result in a more gradual rise of the occupation function from zero to one around M_{\min} . In order to understand the qualitative effect of scatter on our inferred number density of halos that match the clustering of z2SFGs, we have run a series of halo occupation models that were constrained to match the observed correlation function (see e.g. Tinker et al. 2006, for details). In these models both M_{\min} and the amount of scatter between mass and light were left as free parameters. The resulting number density of halos with clustering matching the observed z2SFGs varies by $\sim 20\%$ compared to the number density of halos when setting the scatter to zero (which is our default model herein). The effect of scatter is thus insignificant for our purposes.

Using r_0 to constrain the minimum dark matter halo mass of high-redshift galaxies is not a new technique (e.g. Wechsler et al. 1998). Previously, Adelberger et al. (2005) used the GIF- Λ CDM simulation (Kauffmann et al. 1999) to constrain the minimum mass, finding that $M_{\min} \sim 10^{11.8} h^{-1} M_{\odot}$ provided a good fit to the $z \sim 2$ data (which is the same data used herein). The difference between this value and ours ($10^{11.4} h^{-1} M_{\odot}$) is due to the updated Ω_m and more physically motivated transfer function in the simulations we use.¹² At first glance this may be worrisome, since the cosmology used herein is already somewhat out-dated insofar as the new *WMAP3* results (Spergel et al. 2007) favor a lower normalization of the power spectrum ($\sigma_8 = 0.76$) than what we assume. To explore the dependence of our conclusions on cosmological parameters, we have made use of simulations, described in §2.3, with the updated *WMAP3* parameters and find that the best-fit M_{\min} decreases by 0.3–0.4 dex. This lower M_{\min} results in a 35–70% increase in the abundance of z2SFG host halos — well within the uncertainties associated with matching halos to galaxies using clustering, as discussed above. The differences between the *WMAP1* and *WMAP3* cosmological parameters thus have a small impact on the halo-z2SFG connection.

In sum, the observed clustering strength and comoving number density of z2SFGs combine to suggest that every dark matter halo and subhalo with mass $\geq 10^{11.4} h^{-1} M_{\odot}$ is host to roughly one z2SFG. The subhalo fraction among these halos implies that 11% of z2SFGs are satellites.

Techniques complementary to the optical color-selection method used to identify z2SFGs have identified a population of massive, red galaxies at $z \sim 2$ with low space density (i.e. objects with $n \sim 10^{-4} h^3 \text{ Mpc}^{-3}$; Franx et al. 2003; Daddi et al. 2004; van Dokkum 2006). A significant fraction of these objects may be missed by the z2SFG *UGR* criteria — especially if they have little or no ongoing star-formation. However, since the observed z2SFG sample has a space density of $n \sim 10^{-2} h^3 \text{ Mpc}^{-3}$, our results are not sensitive to this possibly distinct population of massive red galaxies because such ob-

jects are comparatively rare and thus have little impact on the number density and clustering of the overall set of z2SFGs.

3.1.1. Quiescent versus Collisional z2SFGs

In the previous section we found that the number density of halos above M_{\min} was consistent with the observed number density of z2SFGs, given the uncertainty in M_{\min} . Thus, within the uncertainties, all halos above M_{\min} contain one z2SFG. Such a scenario arises naturally if z2SFGs are quiescently forming stars, since in this picture every sufficiently massive halo should have the same conditions necessary for star-formation (e.g. a sufficient supply of cold gas). Here and throughout, “quiescent” refers to an approximately continuous star-formation history, as opposed to an episodic one.

However, it is less clear that a collisional starburst scenario (where star formation is merger-induced and thus episodic) would be consistent with this result, since the majority of halos, at any mass scale, are not undergoing violent mergers frequently enough. For example, based on merger trees in the Millennium simulation, only $\sim 20\%$ of halos above $M_{\min} = 10^{11.4} h^{-1} M_{\odot}$ at $z \sim 2$ have had a merger with mass ratio $< 3 : 1$ in the past gigayear. If elevated star formation occurs for such mergers but not for mergers at larger mass ratios, as suggested by controlled hydrodynamic simulations (e.g. Mihos & Hernquist 1994; Cox et al. 2007), then there are simply too few such mergers in halos with $M \geq M_{\min}$ to explain the abundance of observed z2SFGs under the collisional starburst scenario. Previous modeling efforts (Kolatt et al. 1999; Wechsler et al. 2001) concluded that the collisional starburst scenario was viable because they included collisions with very high mass ratios (10 : 1 and greater). It now appears, however, that such merger ratios will not result in the enhanced star-formation (Cox et al. 2007) necessary to make them detected as z2SFGs. Moreover, the small scatter in the observed star-formation rate-stellar mass relation at $z \sim 1$ suggests that by this epoch starbursts are not the dominant mode of star formation in most galaxies (Noeske et al. 2007).

Of course, to accommodate the low rate of roughly equal mass mergers, one could lower M_{\min} until the number density of halos with low mass-ratio mergers ($< 3 : 1$) matched that of the z2SFGs. However, lowering M_{\min} in order to incorporate more colliding halos would also lower the large scale clustering strength, and would quickly produce disagreement with the observed clustering of z2SFGs (note that any “merger bias”, in the sense that colliding halos are more clustered than other halos of the same mass, is probably small; see Scannapieco & Thacker 2003). Models that rely on collisions as the impetus for star-formation would thus have a very difficult time simultaneously matching the observed clustering and space density of observed z2SFGs.

Some degree of caution is in order when attempting to discriminate between these two scenarios for the origin of z2SFGs, as the accretion and merging rate of halos is significantly higher at high redshift compared to $z \sim 0$, and thus the dichotomy between quiescent and collisional star-formation may not be applicable at high redshift. As noted above, major mergers, which are the types of mergers thought to fuel collisional starbursts, are still sufficiently rare to rule that channel out as a major contributor to the star-formation rate. But minor mergers of ratio $\sim 10 : 1$ are far more common at higher redshift, and far fewer halos are truly quiescent, at least in terms of their accretion of dark matter. For example, the halos above M_{\min} at $z \sim 2$ in the Millennium simulation have a mass doubling time of ~ 1 Gyr; only the rarest and most

¹² The GIF simulations used an analytic fitting function for the power spectrum transfer function (Bond & Efstathiou 1984) while the Millennium simulation utilized the more accurate CMBFAST code (Seljak & Zaldarriaga 1996) to generate it.

massive halos have such vigorous accretion properties today (Wechsler et al. 2002).

3.1.2. The Baryon Budget

Here we briefly compare the available baryon reservoir inferred from our results to estimates of the gas+stellar mass in a subsample of observed z2SFGs.

The average halo mass for the z2SFGs is $10^{11.8} h^{-1} M_{\odot}$; this can be converted into an average *baryonic* mass by assuming that each halo contains the universal baryon fraction, $f_b = 0.17$ (Spergel et al. 2007). Under this assumption, the average baryonic mass for the z2SFG sample is $1.1 \times 10^{11} h^{-1} M_{\odot}$. For a fraction of the z2SFGs modeled in the present work there exist stellar and gas mass estimates (Erb et al. 2006c). The observed gas masses were estimated by utilizing the empirical Kennicutt (1998) law that relates star-formation rate densities to cold gas densities. The star-formation rate was estimated from the $H\alpha$ emission line and its surface density was estimated from the ~ 6 kpc extent of the emission. Stellar masses were estimated from stellar population synthesis modeling with a Chabrier (2003) IMF. The average observed gas+stellar masses of these objects is $5.8 \times 10^{10} M_{\odot}$, for $h = 0.7$.

In order to compare our expected average baryon fraction to this gas+stellar mass estimate we convert our mass to $h = 0.7$ units, and find that the observed gas+stellar mass estimate is roughly a factor of three smaller than the average baryonic mass inferred from the halos. Based on the assumption that the Kennicutt law holds at $z \sim 2$, and thus that the estimated gas masses are accurate, our results indicate that on average a third of the baryons in the halo are in the central ~ 6 kpc. Furthermore, while $> 50\%$ of the *observed* baryons in z2SFGs appear to have been converted into stars (Erb et al. 2006c,a), the inferred baryonic mass from the average z2SFG halo mass indicates that only $\sim 20\%$ of the *total available* baryons have been converted into stars. Moreover, halos are constantly being fed new gas as they accrete gas-filled dark matter halos. There is thus a sufficient supply of gas to sustain star formation for many gigayears, if the gas is able to cool. As we will see below, this feature is important because many of the z2SFG descendants are galaxies that are still forming stars at $z \sim 1$ and $z \sim 0$.

3.2. z2SFG Evolution to $z \sim 1$ and $z \sim 0$

The identification of the halos likely containing z2SFGs is the first step toward understanding the evolution of these galaxies to $z \sim 1$ and $z \sim 0$, where there are well-defined samples such as the Deep Extragalactic Evolutionary Probe 2 (DEEP2; Davis et al. 2003), the VIMOS VLT Deep Survey (VVDS; Le Fèvre et al. 2005), the 2dF Galaxy Redshift Survey (2dFGRS; Colless et al. 2001), and the Sloan Digital Sky Survey (SDSS; Adelman-McCarthy et al. 2006). The next step is to evolve these halos forward in time using the halo merger trees from the Millennium simulation. Note that the merger trees follow the evolution of subhalos until they have been destroyed, i.e., until the halo finder no longer identifies the subhalo as a bound clump of particles.

The primary ambiguity in this next step is how we treat z2SFG subhalos that, according to the merger trees, have merged/disrupted at some later time. These cases are ambiguous because the Millennium simulation may, like any simulation, *artificially* destroy a subhalo, either because of resolution limits (e.g. Moore et al. 1999; Klypin et al. 1999) or because the simulation does not include the effects of baryon

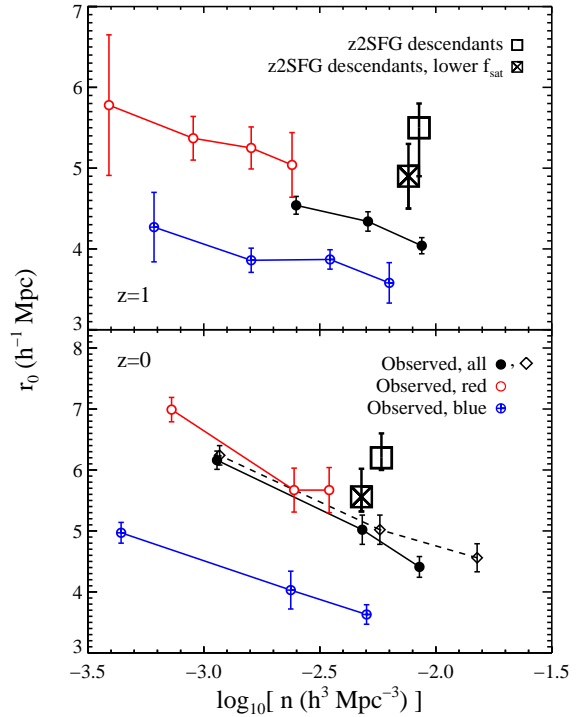


FIG. 2.— Relationship between clustering strength (r_0) and sample number density (n) for observed galaxies and the descendants of the halos hosting z2SFGs at $z \sim 1$ (top panel) and $z \sim 0$ (bottom panel). The data at $z \sim 1$ are for samples defined above various magnitude thresholds (from -19.5 to -20.5 in half magnitude steps for the overall sample, and from -19 to -21 for the color-defined samples; Coil et al. 2006, 2007), while at $z \sim 0$ they are defined for magnitude bins (in one magnitude intervals from -19 to -22 Zehavi et al. 2005). We have also included data from the “all” sample at $z \sim 0$ for magnitude threshold samples (diamonds) in order to show the differences between binned and threshold samples (see §3.2.1 for details). For the halos, error bars encompass the uncertainty due both to M_{min} and the merger vs. no merger scenarios (see §3.2 for details). The location of the symbols for the halos indicates the values for the merger scenario with $M_{\text{min}} = 10^{11.4} h^{-1} M_{\odot}$ (large open boxes). z2SFG descendant halos with a satellite fraction lowered to match observations are also included (large crossed boxes).

condensation, which may make a subhalo more resilient to disruption in the real universe (although the latter effect is expected to be small for the regimes of interest here; see e.g. Nagai & Kravtsov 2005; Weinberg et al. 2006). We incorporate this uncertainty by computing results in this section for two cases that should bracket the range of possibilities. In the first case we assume that the simulation is correct and that when a subhalo merges, so does the galaxy embedded within it. In the second case we assume that none of the subhalos actually merges. In this case, if a subhalo merges within a distinct halo according to the merger tree, we place the satellite within the distinct halo with a position specified by an NFW distribution (Navarro et al. 1997) appropriate for the background dark matter¹³. These will be referred to as the merger and no-merger scenarios below. For reference, the conclusions reached in Adelberger et al. (2005), namely that z2SFGs evolve into massive red galaxies by $z \sim 0$, were based

¹³ In fact, the galaxies associated with disrupted subhalos will likely be more centrally concentrated than the dark matter (Sales et al. 2007). However, the radial distribution of galaxies within the halo has a negligible effect on the large-scale clustering strength and leaves the satellite fraction and number density of the galaxies unchanged. This uncertainty thus does not impact our analysis.

on the no-merger scenario.

In what follows we focus on three constraints that will help discriminate between possible evolutionary histories of z2SFGs; these are the space density of galaxies, their large scale ($1 \lesssim r \lesssim 10 h^{-1}$ Mpc) clustering strength, and the fraction of galaxies that are satellites. These three constraints, when combined, strongly disfavor any scenario where z2SFGs evolve into a single class of objects at lower redshift (i.e. red, blue, central satellite). As we discuss the evolution of z2SFGs to lower redshifts, it is worth remembering that z2SFGs are defined according to a luminosity-limit in the rest-frame UV, while samples at lower redshifts are defined according to increasingly redder rest-frame bands (B -band at $z \sim 1$ and r -band at $z \sim 0$). At increasingly shorter wavelengths, the light emitted by galaxies is increasingly dominated by young stars and hence recent episodes of star-formation, while longer wavelengths are dominated by older stars and hence probe the total stellar mass of a galaxy. At first glance then, connecting galaxies selected by star-formation at $z \sim 2$ to galaxies selected more closely by stellar mass at $z \sim 0$ would seem to be a daunting task. However, with the assignment of z2SFGs to dark matter halos, connecting these galaxies to their lower redshift counterparts becomes simpler thanks to the halo merger trees, which provide a clear connection between high and low redshift.

The space densities, large-scale clustering strengths, and satellite fractions of z2SFG descendants and various observed samples are plotted in Figures 2 and 3. The uncertainties on r_0 and f_{sat} for the z2SFG descendant halos reflect the uncertainty in M_{min} and the uncertain fate of satellites within merged subhalos. In contrast, the uncertainty in the number densities of z2SFG descendant halos reflects the error in the observed z2SFG number density, with the additional uncertainty due to mergers. In other words, the observed z2SFG number density is multiplied by the fraction of z2SFG halos that survive to $z \sim 1$ and $z \sim 0$ in order to deduce the number density of z2SFG descendants at these epochs. The uncertainty in the halo number density due to the uncertainty in M_{min} thus is not included in the uncertainty in the observed z2SFG descendants. After discussing these constraints, we compare the distribution of z2SFG descendant halo masses with the halo masses of observed galaxies at lower redshifts, as inferred from halo occupation modeling. The most basic observational constraint, the abundance of galaxies of various types at multiple epochs, is considered first.

3.2.1. Number Density

In the no-merger scenario, the comoving number density of z2SFGs is constant with time, by construction. Including the possibility of z2SFG mergers (as determined by the merging/disruption of their associated subhalos), results in only mildly more evolution than the no-merger case: by $z \sim 1$ the number density of z2SFG descendant halos is 76% of its $z \sim 2$ value and by $z \sim 0$ it is 53% of that at $z \sim 2$. Recall that our merger prescription associates a z2SFG merger with the merging/disruption of its associated subhalo, which is likely an over-estimate of the true merging because of simulation resolution effects. Nonetheless, if we use the fraction of surviving halos as a proxy for the galaxy number density at lower redshift, more than half of the z2SFGs exist as independent entities at $z \sim 0$.

Figures 2 and 3 plot along the x -axis the number density of z2SFG descendants at $z \sim 1$ and $z \sim 0$. Figure 2 also plots along the x -axis the abundances of observed galaxies

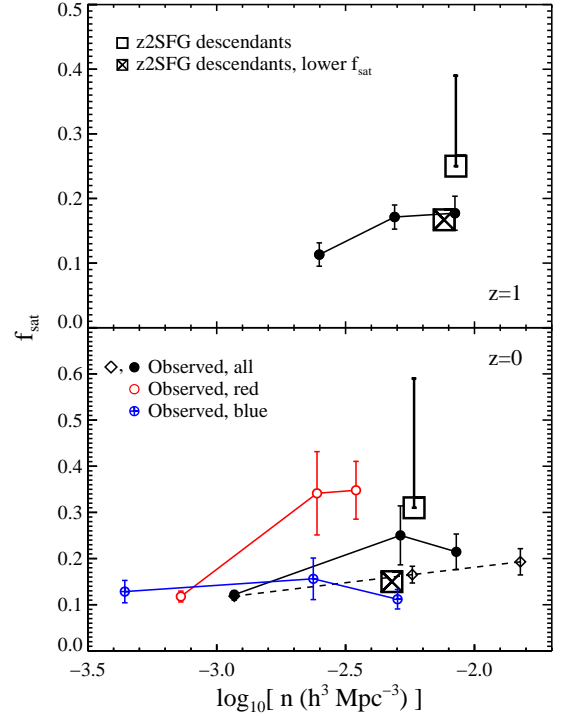


FIG. 3.— Relationship between satellite fraction and sample number density for the z2SFG halo descendants (*large boxes*) and various observations (*circles*; symbols are as in Figure 2), at both $z \sim 1$ (*top panel*) and $z \sim 0$ (*bottom panel*). Also included are z2SFG descendant halos with a satellite fraction measured from the Millennium simulation (*large open boxes*) and lowered to match observations (*large crossed boxes*). For the halos, error bars encompass the uncertainty due both to M_{min} and the merger vs. no merger scenarios (see §3.2 for details). The location of the symbols for the halos indicates the values for the merger scenario with $M_{\text{min}} = 10^{11.4} h^{-1} M_{\odot}$.

as a function of luminosity and color for absolute B -band magnitude thresholds at $z \sim 1$ (in half magnitude steps from -19.5 to -20.5 for the overall sample, and from -19 to -21 for the color-defined samples) and for absolute r -band magnitude bins at $z \sim 0$ (in one magnitude intervals from -19 to -22) based on the luminosity functions at these epochs (Willmer et al. 2006; Bell et al. 2004; Blanton et al. 2003). For reference, at $z \sim 1$ $M_B^* = -20.6$ and at $z \sim 0$ $M_r^* = -20.4$. At both epochs, blue and red galaxies are separated according to the observed bimodal distribution of optical colors (Baldry et al. 2004; Bell et al. 2004). We have also included data at $z \sim 0$ for overall magnitude threshold samples in order to demonstrate the small difference between using magnitude bins and thresholds.¹⁴

The mild evolution of the z2SFG descendant halo number density already places strong constraints on the possible progeny of z2SFGs. It has been proposed that red galaxies are the descendants of z2SFGs. However, there are simply far too many z2SFG descendants compared to the observed number density of $z \sim 1$ red galaxies for this to be the case, even when including rather faint ($M_B = -19.5$) red galaxies. Since the faint-end slope of the red galaxy luminosity function at $z \sim 1$ is shallow ($\alpha = -0.5$; Willmer et al. 2006), the number density of all red galaxies to a limiting magnitude of $M_B = -18.0$ ($4.4 \times 10^{-3} h^3 \text{ Mpc}^{-3}$) still does not equal the

¹⁴ Magnitude bins, rather than thresholds, are used at $z \sim 0$ because r_0 is only available in magnitude bins for the color-defined samples.

abundance of z2SFG descendant halos. The abundance of an overall (i.e. no cut on color) sample of galaxies brighter than $M_B = -20.0$ at $z \sim 1$ is much more similar to the abundance of z2SFG descendant halos. At $z \sim 0$ the conclusions are similar. The observed sample at $z \sim 0$ with the number density closest to the z2SFG descendant number density is the overall $-21 < M_r < -20$ sample.

These conclusions, based solely on the abundances of halos and galaxies, suggest that at most a fraction of z2SFGs have evolved onto the red sequence by either $z \sim 1$ or $z \sim 0$ (see also Moustakas & Somerville 2002; Gilli et al. 2007, who reached similar conclusions). The z2SFGs also do not appear to evolve exclusively into the most luminous ($> L^*$) population of galaxies at either epoch, as the number density of such galaxies is much lower than the descendant halos of z2SFGs. Rather, the abundances of descendant z2SFG halos is most similar to typical $\sim L^*$ galaxies at both $z \sim 1$ and $z \sim 0$.

Previous work by Adelberger et al. (2005) came to the conclusion that by $z \sim 1$ z2SFG descendants had largely evolved into red galaxies. This conclusion was based in part on an earlier estimate of the observed number density of red galaxies at $z \sim 1$ (Chen et al. 2003), which was a factor of several larger than current, more accurate estimates (Willmer et al. 2006). The number density of red galaxies at $z \sim 0$ was similarly somewhat higher than the more recent data used herein (Zehavi et al. 2005). The lower number density of observed z2SFGs used in Adelberger et al. (2005), compared to what we adopt from more recent data, also made it appear in that work that z2SFGs evolved into red galaxies by $z \sim 0$. Our use of more accurate and up-to-date number densities at all epochs is a significant reason why our results are a departure from the conclusions reached by Adelberger et al. (2005).

3.2.2. Clustering Strength

Figure 2 plots the large-scale clustering strength, r_0 , as a function of number density for both observed galaxy samples and z2SFG descendant halos at $z \sim 1$ (top panel) and $z \sim 0$ (bottom panel). The data samples include both overall and color-defined samples, for a range of luminosities described above. The clustering data for these samples come from Coil et al. (2006) and Coil et al. (2007) for $z \sim 1$ and from Zehavi et al. (2005) for $z \sim 0$. For the halos, the power-law fit to the correlation function is computed by solving simultaneously for r_0 and γ over the range $1 < r < 10 h^{-1}$ Mpc. The uncertainty on r_0 for the halos is dominated by the uncertainty on M_{\min} at $z \sim 2$.

From the figure it is clear that the clustering of z2SFG descendant halos is comparable to that of the most luminous red galaxies, at both epochs. This point has been used as evidence that z2SFGs evolve into red galaxies by $z \sim 1$ (e.g. Adelberger et al. 2005). However, as discussed in the previous section, the constraints from the abundance of z2SFG descendants strongly disfavors this scenario. Moreover, r_0 is sensitive to the number of satellite galaxies, and thus should not be used as a constraint without also considering the observed constraints on the satellite fraction.

3.2.3. Satellite Fraction

We now turn to a discussion of the satellite fractions of z2SFG halos and their descendants, and of observed galaxies as inferred from halo occupation modeling. For z2SFG host dark matter halos, the satellite (i.e. subhalo) fraction at $z \sim 2$ is 11%, while at $z \sim 1$ and $z \sim 0$ it is 24–39% and 31–59%,

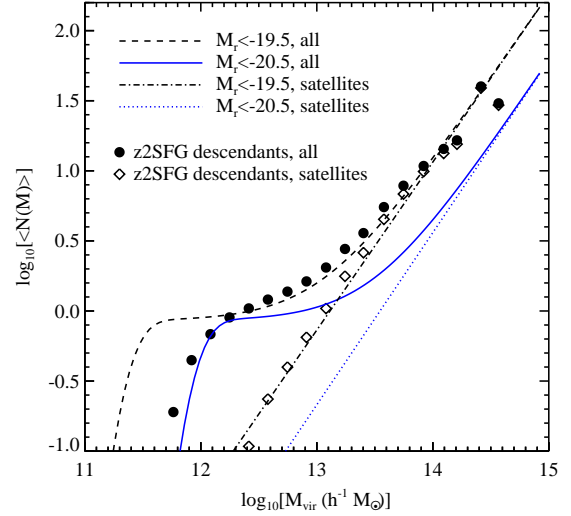


FIG. 4.— The average number of z2SFG descendants per distinct halo at $z \sim 0$ as a function of distinct halo mass for the overall descendant sample (filled circles) and for the satellites only (diamonds). These results are compared to the average number of galaxies per halo as inferred from halo occupation modeling, for all galaxies with magnitudes $M_r < -20.5$ and $M_r < -19.5$, and for satellites only.

respectively. The lower and upper bounds in satellite fraction depend primarily on the assumption of merging or no merging of the satellites within destroyed subhalos. Figure 3 compares these satellite fractions to satellite fractions derived for various data sets at $z \sim 1$ (Zheng et al. 2007)¹⁵ and $z \sim 0$. The derived satellite fractions were estimated by simultaneously fitting the observed number densities and projected two-point correlation functions of the galaxy samples with halo occupation models (see e.g. Tinker et al. 2005; Zheng et al. 2007, for details). The satellite fractions for the color-defined samples at $z \sim 0$ are reported here for the first time.

From this plot it is clear that the z2SFG descendant halos have higher satellite fractions than any overall luminosity-limited sample at either $z \sim 1$ or $z \sim 0$ (except perhaps the faintest sample at $z \sim 0$). Only the fainter ($-21 < M_r < -19$) red galaxy samples at $z \sim 0$ have comparable satellite fractions. On the other hand, these faint red galaxies have large-scale clustering strengths that are lower than the z2SFG descendant halos (Figure 2) and they are thus not the likely descendants of z2SFGs. The satellite fraction of z2SFG descendants is higher than that of a typical mass-selected sample of halos because, while the sample is mass-selected at $z \sim 2$, it is not mass-selected at lower redshifts due to the different evolutionary histories of subhalos and distinct halos (described in more detail in §3.2.5).

In order to better illustrate how the satellite fraction and clustering strengths are related, we lower the satellite fractions of the z2SFG descendant halos at $z \sim 1$ and $z \sim 0$ so that they agree with the observed satellite fractions of $\sim L^*$ galaxies at both epochs. We do this by removing a fraction of the oldest subhalos (i.e. those subhalos that accreted at the highest redshifts) such that the resulting halo satellite fractions are 17% at $z \sim 1$ and 15% at $z \sim 0$. In other words, at

¹⁵ Zheng et al. (2007) define a halo to be the mass enclosed within a region 200 times the mean density of the Universe (rather than the critical density as is used herein), and so their satellite fractions will be somewhat larger than those calculated using our halo definition.

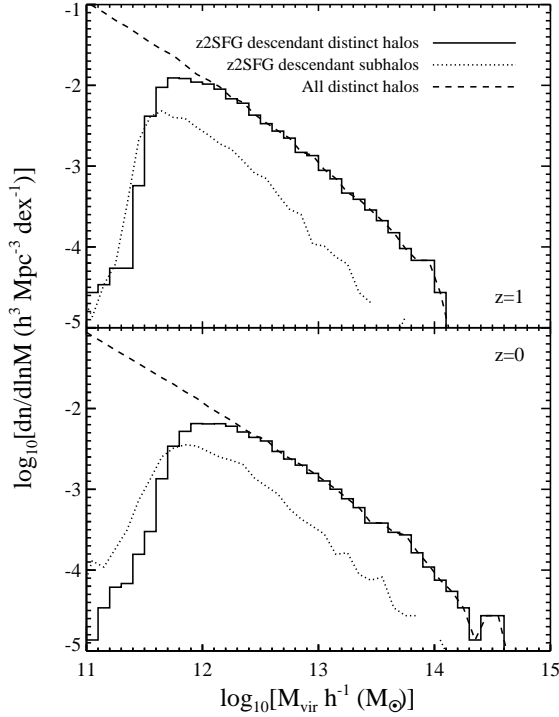


FIG. 5.— Mass function for z2SFG distinct halo descendants (*solid line*), z2SFG subhalo descendants (*dotted line*), and all distinct halos (*dashed line*), at $z \sim 1$ (*top panel*) and $z \sim 0$ (*bottom panel*), not including subhalos. For subhalos, the mass refers to the mass it had at the epoch of accretion. Note that for masses $\gtrsim 10^{12} h^{-1} M_{\odot}$ the halos that contained z2SFGs constitute the vast majority of all halos above this mass at $z \sim 1$ and $z \sim 0$.

$z \sim 0$ we have removed 60% of available z2SFG descendant satellites. As seen in Figure 2, it is clear that the clustering of the z2SFG descendant halos with lower satellite fractions is in much better agreement with the clustering of observed overall $\sim L^*$ galaxies at both epochs. This result is not strongly affected by removing the oldest subhalos as opposed to a random set; we remove the oldest because it is these subhalos that are most likely to have faded significantly in luminosity, and thus may plausibly not be included in a sample of $\sim L^*$ galaxies at lower redshift. Moreover, reducing the satellite fraction to zero results in r_0 values of 4.2 and $4.9 h^{-1}$ Mpc at $z \sim 1$ and $z \sim 0$, respectively. These numbers bracket the observed values near $\sim L^*$. The implications of this exercise are discussed more fully in the sections that follow.

3.2.4. Insights from Halo Occupation Modeling

Halo occupation modeling has emerged as a powerful tool to analyze observational data (e.g. Seljak 2000; Berlind & Weinberg 2002; Scoccimarro et al. 2001; Bullock et al. 2002; Kravtsov et al. 2004; Zehavi et al. 2005; Tinker et al. 2005; Cooray 2006; Tinker et al. 2007; Zheng et al. 2007; van den Bosch et al. 2007). The model quantifies the statistical distribution of galaxies within dark matter halos, specifying the probability that a halo of mass M contains N galaxies of a particular type. A given halo occupation distribution maps nearly uniquely onto a two-point correlation function, so the occupation function can be constrained by clustering measurements. In the context of this model, “halos” refers only to distinct halos, and not the subhalos within them.

The function $\langle N(M) \rangle$ specifies the mean number of galaxies in a halo of mass M and is typically split into two terms, one describing the number of central galaxies, $\langle N_c \rangle$, and the other describing satellite galaxies, $\langle N_s \rangle$ (the dependence on halo mass is implicit in these functions). When constraining $\langle N(M) \rangle$, the approach taken is to assume that $\langle N_c \rangle$ rises from zero to one at some mass scale, with a rapidity constrained by the data. The number of central galaxies never rises above one by definition. The number of satellite galaxies is taken to be a power-law in halo mass, $\langle N_s \rangle \propto M^\alpha$, where α is usually found to be near unity. This form is well-motivated both by results from hydrodynamic (Zheng et al. 2005) and dissipationless simulations (Kravtsov et al. 2004), and observations (e.g. Lin et al. 2004). Details of the halo occupation results presented in this section can be found in Tinker et al. (2005), Tinker et al. (2006), and Tinker et al. (2007), although the fits presented herein are new because they utilize a halo mass definition that is identical to the mass definition used throughout the rest of this paper – the mass enclosed within a region that is 200 times the critical density of the Universe.

Figure 4 plots the $\langle N(M) \rangle$ that best matches the abundance and clustering of observed galaxies from the SDSS survey with magnitudes $M_r < -20.5$ and $M_r < -19.5$ at $z \sim 0$. The figure shows explicitly the contribution of satellites to the full $\langle N(M) \rangle$. The contribution due to centrals can be inferred by subtracting the satellite contribution from the total. These results are compared to the average number of z2SFG descendants per halo, where the contribution due to z2SFG descendants that are satellites is also included.

It is clear that $\langle N(M) \rangle$ for the z2SFG descendants that are satellites by $z \sim 0$ agrees very well with that of observed satellite galaxies with $M_r < -19.5$. Moreover, the fact that the overall $\langle N(M) \rangle$ for z2SFG descendants drops rapidly to zero at roughly the same mass scale as observed galaxies with $M_r < -20.5$ indicates that the z2SFGs that are central galaxies by $z \sim 0$ correspond closely to galaxies with $M_r < -20.5$. This last fact follows because the region where $\langle N(M) \rangle \lesssim 1$ is dominated by central galaxies. Scatter in the relation between halo mass and UV luminosity at $z \sim 2$, as discussed in §3.1, will produce a softer roll off in $\langle N(M) \rangle$ at lower masses for the z2SFG descendants than what is shown in Figure 4. The effect of scatter is thus to associate a fraction of z2SFG descendants that are centrals with galaxies fainter than $M_r = -20.5$. However, as discussed in §2.1, the scatter is not expected to be substantial because of the observed UV-luminosity-dependent clustering observed at $z \sim 2$.

This comparison vividly demonstrates that z2SFG descendants that are satellites by $z \sim 0$ evolve into observed faint, $M_r < -19.5$, galaxies, while those descendants that remain distinct halos (i.e. central galaxies) evolve into more luminous, $M_r < -20.5$, galaxies. Echoing the conclusions drawn from previous sections, it is clear from this figure that z2SFG descendants do not generically evolve into a single class of galaxies at later epochs. Rather, the evolution of z2SFG descendants that become satellites is qualitatively different from those that become central galaxies.

The ratio between $\langle N_s \rangle$ for galaxies brighter than $M_r = -20.5$ and $M_r = -19.5$ is $\sim 30\%$, indicating that approximately 30% of galaxies brighter than $M_r = -19.5$ are also brighter than $M_r = -20.5$. In §3.2.3 we found that keeping only 40% of the total number of z2SFG descendants that are satellites yielded a sample of z2SFG descendants that had both clustering strengths, satellite fractions, and abundances in good agreement with the observed sample of galaxies at $z \sim 0$ with

$M_r \lesssim -20$. The fact that these fractions are similar suggests a physical motivation for reducing the satellite fraction of the z2SFG descendants in order to produce better agreement with an observed $z \sim 0$ sample defined with respect to a luminosity cut. A large fraction of z2SFG descendants that become satellites are faint, and so the overall sample of z2SFG descendants, which includes these faint satellites, will not compare to any observed sample of galaxies defined according to a simple luminosity cut.

3.2.5. Descendant Halo Masses

Finally, we turn to a discussion of the mass distribution of halos hosting z2SFG descendants at lower redshifts. Figure 5 plots the mass function of distinct z2SFG descendant halos at $z \sim 1$ and $z \sim 0$ and compares to the full mass function of distinct halos from the simulation. It is clear that z2SFG descendant halos with mass $\gtrsim 10^{12} h^{-1} M_\odot$ constitute the vast majority of all halos in that mass range at $z \sim 1$ and $z \sim 0$. In other words, virtually all halos today with mass $\gtrsim 10^{12} h^{-1} M_\odot$ contained at least one z2SFG. In light of this fact, it thus appears that the descendants of z2SFGs are not only the galaxies at the centers of massive halos but rather constitute a wide variety of objects in a variety of environments. In fact, by far the most common place to find the descendants of z2SFGs at $z \sim 0$ is in $\sim 10^{12} h^{-1} M_\odot$ halos.

It is furthermore clear from the figure that the average mass of distinct z2SFG descendant halos is growing modestly with time. At $z \sim 2$ the average distinct halo mass is $10^{11.8} h^{-1} M_\odot$, at $z \sim 1$ it has increased to $10^{12.1} h^{-1} M_\odot$ and by $z \sim 0$ it is $10^{12.3} h^{-1} M_\odot$. Note that these average masses are not weighted by the number of satellites/subhalos within each distinct halo.

Figure 5 also includes the mass function of z2SFG descendants that are subhalos by $z \sim 1$ and $z \sim 0$. Here the subhalo mass is measured at the epoch of accretion. Aside from the obvious fact that the subhalos constitute only a fraction (f_{sat}) of the total halo population, the mass function of these subhalos clearly peaks at a lower mass than for the distinct descendant halos. This is not surprising given the fact, for example, that the average redshift of accretion for subhalos identified at $z \sim 0$ is $z \approx 0.5$. The mass that these subhalos had at the epoch of accretion is on average only 55% of the average mass of $z \sim 0$ z2SFG descendant halos that are not subhalos. Thus, in the $\sim 3.5 h^{-1}$ Gyr since $z \approx 0.5$, z2SFG descendants residing at the centers of distinct halos continued to grow, both in dark matter, gas, and presumably in stars (via star formation), while those in subhalos did not grow in dark matter or gas, and were likely subject to one or more gas-starvation processes, thereby further halting the growth of the galaxy embedded within the subhalo. This difference between z2SFG descendants that are subhalos and those that are distinct halos has significant implications for the galaxies likely embedded within them.

3.2.6. Sensitivity to Cosmological Parameters

As discussed in §3.1, we have made use of an N -body simulation run with cosmological parameters advocated by the *WMAP3* results (Spergel et al. 2007) in order to assess the sensitivity of our results to these new parameters. In §3.1 we found that the halos in the *WMAP3* cosmology with clustering most similar to observed z2SFGs have M_{min} lower by 0.3–0.4 dex compared to the *WMAP1* cosmology. However, once we have identified a population of halos with comparable clus-

tering to the observed population in both cosmologies, their subsequent evolution to lower redshift is almost identical. In particular, we have followed the evolution of distinct halos (not subhalos) in the *WMAP3* cosmology and find that r_0 of the descendants is 5–10% lower compared to the *WMAP1* cosmology at both $z \sim 1$ and $z \sim 0$. Furthermore, the fraction of halos that merged away by $z \sim 1$ and $z \sim 0$ differs by less than 5% for the two cosmologies. Note that since we use the observed number density of z2SFGs multiplied by the fraction of halos that survive to later epochs, rather than the number density of halos themselves, our quoted number densities of descendants are insensitive to cosmological parameters (see §3.2 for more details). The differences between these two cosmologies thus has a negligible impact on our conclusions regarding the descendants of z2SFGs.

4. DISCUSSION

In the preceding section we found that the observed abundance and clustering of z2SFGs implied that every halo at $z \sim 2$ above a mass of $10^{11.4} h^{-1} M_\odot$ contains one z2SFG. By $z \sim 0$, the overall population of halos that once hosted z2SFGs, and survived to $z \sim 0$, has a comoving number density comparable to that of $\sim L^*$ galaxies ($M_r \lesssim -20$; while $M_r^* = -20.4$), a clustering strength comparable to luminous ($M_r \lesssim -21$) red galaxies, and a satellite fraction comparable to $\sim L^*$ or fainter red galaxies. We found that a subsample of z2SFG descendant halos where 60% of the satellites were removed resulted in much better agreement with the clustering strength, satellite fraction, and number density of $\sim L^*$ galaxies at $z \sim 0$. Comparison to halo occupation modeling of observed galaxy samples revealed that the z2SFG descendants that are central galaxies most closely resemble observed galaxies brighter than $M_r \sim -20.5$ while the satellite properties compare more favorably to galaxies brighter than $M_r \sim -19.5$. The average redshift at which z2SFG descendant satellites at $z \sim 0$ were accreted onto their parent halo was $z \approx 0.5$, and the mass of the halo associated with these satellites when they were accreted was only 55% of the mass of distinct halos at $z \sim 0$, on average. This indicates that the growth of subhalos (and the galaxies within them) was significantly less than that of distinct halos.

These results have straightforward implications regarding the connection between z2SFGs and their descendants at $z \sim 0$. First, it is abundantly clear that z2SFGs do not evolve into any single sample of galaxies defined either according to a luminosity cut or a luminosity and color cut. In particular, they do not evolve exclusively into massive red galaxies, either by $z \sim 1$ or $z \sim 0$. Rather, the subsequent evolution of z2SFGs is more nuanced. Merger trees extracted from simulations indicate that the number density of z2SFG descendants at $z \sim 0$ is $\sim 50\%$ of the number density of z2SFGs because some descendants merge together between $z \sim 2$ and $z \sim 0$. This is an upper bound on the evolution of the number density because halos in our simulations can merge or disrupt without the subsequent merger or disruption of the galaxy within it due to simulation resolution effects or possible baryonic effects. Of the remaining descendants, $\sim 70\%$ are centrals and $\sim 30\%$ are satellites. The central galaxies have properties similar to observed galaxies with $M_r \lesssim -20.5$. In particular, they reside predominantly in halos with mass $M \gtrsim 10^{12} h^{-1} M_\odot$.

An anecdotal consequence is that our own Galaxy, with halo mass $\sim 10^{12} h^{-1} M_\odot$ (Klypin et al. 2002), was once likely a z2SFG. This conclusion is in accord with various properties of the bulge of our Galaxy. For example, the bulge has

a stellar mass of $\sim 10^{10} M_{\odot}$ that is thought to have formed over a short period of time (< 1 Gyr) roughly 10 Gyr ago (Zoccali et al. 2003; Ferreras et al. 2003). These facts imply that the star-formation rate during the formation of the bulge was $> 10 M_{\odot} \text{ yr}^{-1}$. The epoch of formation of the bulge and its high star-formation rate imply that it would have likely been detected as a zSFG (see also Pettini 2006, who reached similar conclusions).

In contrast, the zSFG descendants that become satellites by $z \sim 0$ are much more similar to a fainter sample of observed galaxies ($M_r \lesssim -19.5$). This is not surprising in light of the different histories of satellite compared to central galaxies as inferred from the histories of their dark matter halos. Since satellites fell into their parent halo on average at $z \approx 0.5$ ($3.5 h^{-1}$ Gyr ago), their growth was significantly retarded relative to central galaxies. Satellites grew less not only because they could not accrete new gas but also because the gas they possessed at infall was likely prohibited from cooling to form stars (or removed altogether) due to one or more quenching processes, such as gas strangulation, harassment, or ram-pressure stripping.

Not all satellites are required to be so faint; our results indicate that $\sim 40\%$ are brighter than $M_r \sim -20.5$. It is plausible that the $\sim 60\%$ required to have $-19.5 \lesssim M_r \lesssim -20.5$ were the satellites accreted at the earliest epochs, because such satellites would have the least amount of growth between $z \sim 2$ and $z \sim 0$. Simulated star-formation histories coupled with a stellar population synthesis code (Bruzual & Charlot 2003) confirm that galaxies with properties similar to zSFGs can easily evolve into galaxies with $M_r \sim -19.5$ if their star-formation is truncated at $z \sim 0.5 - 1$. For example, a galaxy at $z \sim 2$ with stellar mass $10^{10} h^{-2} M_{\odot}$ and a star-formation rate of $10 M_{\odot} \text{ yr}^{-1}$ that steadily declines to zero at $z \sim 1$ fades from $M_r = -21.5$ to $M_r = -19.2$ by $z \sim 0$.

Similar conclusions hold for the descendant halos at $z \sim 1$. In particular, from analysis of the Millennium simulation merger trees we find that $\sim 25\%$ of zSFG descendants have merged away by this time. Of the remaining halos, $\sim 25\%$ are satellites and $\sim 75\%$ are central galaxies. If half of the satellites are fainter than $\sim L^*$, then the remaining descendant halos that are satellites and centrals have a number density, clustering strength, and satellite fraction comparable to observed $\sim L^*$ galaxies at $z \sim 1$.

There has been some debate in the literature over whether or not the optical color selection technique used to select zSFGs misses a significant population of redder (i.e. older and/or dustier) galaxies (e.g. Franx et al. 2003; Daddi et al. 2004; van Dokkum 2006; Smail et al. 2002). Under our assumption of a tight correlation between rest-frame UV luminosity and halo mass, we have demonstrated that at $z \sim 2$ roughly every halo with mass above $10^{11.4} h^{-1} M_{\odot}$ contains one zSFG. It would be rather surprising if each halo also contained another comparably massive galaxy not detectable with the optical color selection technique, if only by analogy with lower redshift, where the vast majority of $\sim L^*$ galaxies live alone in their dark matter halos (e.g. Zheng et al. 2007). Thus, while there may well be a population of massive ($M_* \gtrsim 10^{11} h^{-2} M_{\odot}$), red galaxies with a correspondingly low space density ($\sim 10^{-4} h^3 \text{ Mpc}^{-3}$), that is missed with the optical color selection technique (Franx et al. 2003; Daddi et al. 2004; van Dokkum 2006), it is hard to imagine that this could be the case at lower galaxy masses. Since our conclusions are most sensitive to lower mass galaxies, they are not influenced

by this possible distinct population of more massive, less numerous, red galaxies.

There are two basic facts about dark matter halos and their evolution that, when combined, provide both a qualitative understanding of our results and more general insights into the evolution of populations of galaxies across time. The first fact is that, to within a factor of ~ 2 , the space density of a set of halos above a mass threshold does not change from high redshift to the present. For example, of the halos with $M \geq 10^{11.4} h^{-1} M_{\odot}$ at $z \sim 2$, 50% survive to $z \sim 0$. For halos more massive than $10^{11.9} h^{-1} M_{\odot}$ and $10^{12.4} h^{-1} M_{\odot}$ at $z \sim 2$, the fraction that survive to $z \sim 0$ increases to 60% and 70%, respectively. The second fact is that, by and large, the ranking of halos by mass is preserved as the Universe evolves. For example, the most massive halos at $z \sim 2$ evolve to the most massive halos today. If, as we have argued, the zSFGs are an at least approximately halo mass selected sample, then these two basic facts make less surprising the conclusion that zSFGs evolve largely into a roughly halo mass selected sample of abundant galaxies at $z \sim 0$. As described above, it is primarily the uncertain evolution of satellite galaxies that complicates this simple description.

These facts can also shed light on the likely descendants of the massive red galaxies discussed above. If such galaxies are in the most massive halos (as suggested by their high stellar mass and clustering strength; Quadri et al. 2007), then it is these galaxies that will evolve, largely intact, to the centers of rich groups and clusters by $z \sim 0$. Better constraints on the clustering and abundances of these observed massive red galaxies are required to make more detailed statements.

Finally, these basic facts can connect our discussion herein to the fates of star-forming galaxies at $z > 2$. Indeed, much of the previous high-redshift modeling efforts discussed in the Introduction focused on star-forming galaxies at $z \sim 3$, the so-called Lyman-Break Galaxies (LBGs). If we apply our methods to match the observed clustering of LBGs ($r_0 = 4.0 \pm 0.6 h^{-1} \text{ Mpc}$; Adelberger et al. 2005) with a set of halos in the Millennium simulation above some minimum mass, we find a best-fit $M_{\text{min}} = 10^{11.1 \pm 0.2} h^{-1} M_{\odot}$. Analysis of the zSFG halo merger trees indicates that every zSFG halo contains one or more of these LBG halos in their history and approximately 70% of LBGs evolve into zSFGs (in agreement with earlier work; e.g. Adelberger et al. 2005). While the link between LBGs and zSFGs appears strong, there are important subtleties one must keep in mind when comparing LBGs to zSFGs. In particular, the clustering of these two populations has been measured for all objects above a common apparent magnitude limit ($R = 25.5$), and thus the LBGs, being more distant, are an intrinsically more luminous sample compared to the zSFGs. However, the luminosity functions of these two classes of galaxies are nearly the same (Reddy et al. 2007), suggesting that if the two samples were defined with respect to the same absolute luminosity limit, their evolutionary bond would be even stronger. Nonetheless, the clear link between LBGs and zSFGs implies that LBGs share the same varied fates as those we have outlined for zSFGs.

The most significant uncertainty in our analysis is the clustering strength of zSFGs and the subsequent merging of their descendants. A more quantitative understanding of the fate of these zSFGs will thus require a more accurate accounting of their clustering strengths, on the observational side, and a more sophisticated treatment of zSFG mergers on the theoretical side. In addition, clustering measurements on smaller

scales ($\lesssim 1\text{Mpc}$) and over a range of rest-frame luminosities will allow a more detailed modeling of the connection between z2SFGs and halos at $z \sim 2$ than has been presented here and will provide a critical test of our assumption of a tight correlation between rest-frame UV luminosity and halo mass at $z \sim 2$.

With more accurate data over the interval $0 \lesssim z \lesssim 2$, the goal will ultimately be to model the galaxy-halo connection as a function of galaxy properties such as color and luminosity, or star-formation rate and stellar mass, in narrow redshift intervals. The galaxy-halo connections at higher redshift can then be evolved into the connections at lower redshift with the aid of halo merger trees. The merger trees are the key to this approach, as they put the static (fixed redshift) halo occupation models into motion. Such an approach has only recently become feasible, due both to the vastly increased data at these epochs and to a converging set of cosmological parameters that removes significant uncertainties in the properties and histories of dark matter halos (see e.g. Zheng et al. 2007; White et al. 2007; Conroy et al. 2007). A simplified version of this approach has been explored in the present work. A more detailed version will be pursued elsewhere.

We thank Alison Coil, Eric Hayashi, Idit Zehavi, and Zheng Zheng for providing and assisting in the interpretation of their data and results. We also thank J  r  my Blaizot, Alison Coil, Gabriella De Lucia, Andrey Kravtsov, Jerry Ostriker, Max Pettini, Ryan Quadri, Risa Wechsler, Martin White, and Simon White for numerous helpful comments on an earlier draft. AES thanks Guinevere Kauffmann, J  r  my Blaizot and Gabriella De Lucia for their generous hospitality at the Max Planck Institute for Astrophysics, and acknowledges support from the David and Lucile Packard Foundation and the Alfred P. Sloan Foundation. GL works for the German Astrophysical Virtual Observatory (GAVO), which is supported by a grant from the German Federal Ministry of Education and Research (BMBF) under contract 05 AC6VHA. The Millennium Simulation databases used in this paper and the web application providing online access to them were constructed as part of the activities of the German Astrophysical Virtual Observatory. This work made extensive use of the NASA Astrophysics Data System and of the `astro-ph` preprint archive at `arXiv.org`.

REFERENCES

- Adelberger, K. L. & Steidel, C. C. 2000, *ApJ*, 544, 218
 Adelberger, K. L., Steidel, C. C., Pettini, M., Shapley, A. E., Reddy, N. A., & Erb, D. K. 2005, *ApJ*, 619, 697
 Adelberger, K. L., Steidel, C. C., Shapley, A. E., Hunt, M. P., Erb, D. K., Reddy, N. A., & Pettini, M. 2004, *ApJ*, 607, 226
 Adelberger, K. L., Steidel, C. C., Shapley, A. E., & Pettini, M. 2003, *ApJ*, 584, 45
 Adelman-McCarthy, J. K. et al. 2006, *ApJS*, 162, 38
 Baldry, I. K., Glazebrook, K., Brinkmann, J., Ivezi  , Z., Lupton, R. H., Nichol, R. C., & Szalay, A. S. 2004, *ApJ*, 600, 681
 Baugh, C. M., Cole, S., Frenk, C. S., & Lacey, C. G. 1998, *ApJ*, 498, 504
 Bell, E. F. et al. 2004, *ApJ*, 608, 752
 Berlind, A. A. & Weinberg, D. H. 2002, *ApJ*, 575, 587
 Berrier, J. C., Bullock, J. S., Barton, E. J., Guenther, H. D., Zentner, A. R., & Wechsler, R. H. 2006, *ApJ*, 652, 56
 Blaizot, J., Guiderdoni, B., Devriendt, J. E. G., Bouchet, F. R., Hatton, S. J., & Stoehr, F. 2004, *MNRAS*, 352, 571
 Blanton, M., Cen, R., Ostriker, J. P., Strauss, M. A., & Tegmark, M. 2000, *ApJ*, 531, 1
 Blanton, M. R. et al. 2003, *ApJ*, 592, 819
 Bond, J. R. & Efstathiou, G. 1984, *ApJ*, 285, L45
 Bower, R. G., Benson, A. J., Malbon, R., Helly, J. C., Frenk, C. S., Baugh, C. M., Cole, S., & Lacey, C. G. 2006, *MNRAS*, 370, 645
 Bruzual, G. & Charlot, S. 2003, *MNRAS*, 344, 1000
 Bullock, J. S., Wechsler, R. H., & Somerville, R. S. 2002, *MNRAS*, 329, 246
 Cattaneo, A. et al. 2007, *MNRAS*, 377, 63
 Chabrier, G. 2003, *PASP*, 115, 763
 Chen, H.-W. et al. 2003, *ApJ*, 586, 745
 Coil, A. L., Newman, J. A., Cooper, M. C., Davis, M., Faber, S. M., Koo, D. C., & Willmer, C. N. A. 2006, *ApJ*, 644, 671
 Coil, A. L. et al. 2007, *ArXiv:0708.0004*
 Cole, S., Lacey, C. G., Baugh, C. M., & Frenk, C. S. 2000, *MNRAS*, 319, 168
 Coles, P., Lucchin, F., Matarrese, S., & Moscardini, L. 1998, *MNRAS*, 300, 183
 Col  n, P., Klypin, A. A., Kravtsov, A. V., & Khokhlov, A. M. 1999, *ApJ*, 523, 32
 Colless, M. et al. 2001, *MNRAS*, 328, 1039
 Conroy, C., Wechsler, R. H., & Kravtsov, A. V. 2006, *ApJ*, 647, 201
 —. 2007, *ApJ*, 668, 826
 Cooray, A. 2006, *MNRAS*, 365, 842
 Cox, T. J., Jonsson, P., Somerville, R. S., Primack, J. R., & Dekel, A. 2007, *ArXiv:0709.3511*
 Crain, R. A., Eke, V. R., Frenk, C. S., Jenkins, A., McCarthy, I. G., Navarro, J. F., & Pearce, F. R. 2007, *MNRAS*, 377, 41
 Croton, D. J. et al. 2006, *MNRAS*, 365, 11
 Daddi, E., Cimatti, A., Renzini, A., Fontana, A., Mignoli, M., Pozzetti, L., Tozzi, P., & Zamorani, G. 2004, *ApJ*, 617, 746
 Davis, M. et al. 2003, in *Proc. SPIE*, Volume 4834, pp. 161-172 (2003), 161-172
 Dekel, A. & Birnboim, Y. 2006, *MNRAS*, 368, 2
 Erb, D. K., Shapley, A. E., Pettini, M., Steidel, C. C., Reddy, N. A., & Adelberger, K. L. 2006a, *ApJ*, 644, 813
 Erb, D. K., Steidel, C. C., Shapley, A. E., Pettini, M., Reddy, N. A., & Adelberger, K. L. 2006b, *ApJ*, 647, 128
 —. 2006c, *ApJ*, 646, 107
 Ferreras, I., Wyse, R. F. G., & Silk, J. 2003, *MNRAS*, 345, 1381
 F  rster Schreiber, N. M. et al. 2006, *ApJ*, 645, 1062
 Franx, M. et al. 2003, *ApJ*, 587, L79
 Gawiser, E. et al. 2007, *ApJ*, 671, 278
 Giavalisco, M. & Dickinson, M. 2001, *ApJ*, 550, 177
 Gilli, R. et al. 2007, *A&A*, 475, 83
 Governato, F., Baugh, C. M., Frenk, C. S., Cole, S., Lacey, C. G., Quinn, T., & Stadel, J. 1998, *Nature*, 392, 359
 Governato, F., Ghigna, S., Moore, B., Quinn, T., Stadel, J., & Lake, G. 2001, *ApJ*, 547, 555
 Hamana, T., Yamada, T., Ouchi, M., Iwata, I., & Kodama, T. 2006, *MNRAS*, 369, 1929
 Hatton, S., Devriendt, J. E. G., Ninin, S., Bouchet, F. R., Guiderdoni, B., & Vibert, D. 2003, *MNRAS*, 343, 75
 Heinis, S. et al. 2007, *ArXiv:0706.1076*
 Kauffmann, G., Colberg, J. M., Diaferio, A., & White, S. D. M. 1999, *MNRAS*, 303, 188
 Kennicutt, Jr., R. C. 1998, *ApJ*, 498, 541
 Kere  , D., Katz, N., Weinberg, D. H., & Dav  , R. 2005, *MNRAS*, 363, 2
 Klypin, A., Gottl  ber, S., Kravtsov, A. V., & Khokhlov, A. M. 1999, *ApJ*, 516, 530
 Klypin, A., Zhao, H., & Somerville, R. S. 2002, *ApJ*, 573, 597
 Kolatt, T. S. et al. 1999, *ApJ*, 523, L109
 Kravtsov, A. V. & Klypin, A. A. 1999, *ApJ*, 520, 437
 Kravtsov, A. V. et al. 2004, *ApJ*, 609, 35
 Le F  vre, O. et al. 2005, *A&A*, 439, 845
 Lee, K.-S., Giavalisco, M., Gnedin, O. Y., Somerville, R. S., Ferguson, H. C., Dickinson, M., & Ouchi, M. 2006, *ApJ*, 642, 63
 Lin, Y.-T., Mohr, J. J., & Stanford, S. A. 2004, *ApJ*, 610, 745
 Lowenthal, J. D. et al. 1997, *ApJ*, 481, 673
 Mandelbaum, R., Seljak, U., Kauffmann, G., Hirata, C. M., & Brinkmann, J. 2006, *MNRAS*, 368, 715
 Martini, P. & Weinberg, D. H. 2001, *ApJ*, 547, 12
 Meneux, B. et al. 2006, *A&A*, 452, 387
 Mihos, J. C. & Hernquist, L. 1994, *ApJ*, 425, L13
 Mo, H. J. & Fukugita, M. 1996, *ApJ*, 467, L9
 Mo, H. J., Mao, S., & White, S. D. M. 1999, *MNRAS*, 304, 175

- Moore, B., Ghigna, S., Governato, F., Lake, G., Quinn, T., Stadel, J., & Tozzi, P. 1999, *ApJ*, 524, L19
- Moustakas, L. A. & Somerville, R. S. 2002, *ApJ*, 577, 1
- Nagai, D. & Kravtsov, A. V. 2005, *ApJ*, 618, 557
- Navarro, J. F., Frenk, C. S., & White, S. D. M. 1997, *ApJ*, 490, 493
- Noeske, K. G. et al. 2007, *ApJ*, 660, L43
- Ouchi, M. et al. 2005, *ApJ*, 635, L117
- Peterson, J. R., Kahn, S. M., Paerels, F. B. S., Kaastra, J. S., Tamura, T., Bleeker, J. A. M., Ferrigno, C., & Jernigan, J. G. 2003, *ApJ*, 590, 207
- Pettini, M. 2006, in *The Fabulous Destiny of Galaxies: Bridging Past and Present*, ed. V. Le Brun, A. Mazure, S. Arnouts, & D. Burgarella, 319
- Pettini, M., Shapley, A. E., Steidel, C. C., Cuby, J.-G., Dickinson, M., Moorwood, A. F. M., Adelberger, K. L., & Giavalisco, M. 2001, *ApJ*, 554, 981
- Pollo, A. et al. 2006, *A&A*, 451, 409
- Quadri, R. et al. 2007, *ApJ*, 654, 138
- Reddy, N. A., Steidel, C. C., Fadda, D., Yan, L., Pettini, M., Shapley, A. E., Erb, D. K., & Adelberger, K. L. 2006, *ApJ*, 644, 792
- Reddy, N. A., Steidel, C. C., Pettini, M., Adelberger, K. L., Shapley, A. E., Erb, D. K., & Dickinson, M. 2007, *ArXiv:0706.4091*
- Sales, L. V., Navarro, J. F., Lambas, D. G., White, S. D. M., & Croton, D. J. 2007, *MNRAS*, 382, 1901
- Scannapieco, E. & Thacker, R. J. 2003, *ApJ*, 590, L69
- Scoccimarro, R., Sheth, R. K., Hui, L., & Jain, B. 2001, *ApJ*, 546, 20
- Seljak, U. 2000, *MNRAS*, 318, 203
- Seljak, U. & Zaldarriaga, M. 1996, *ApJ*, 469, 437
- Shapley, A. E., Steidel, C. C., Adelberger, K. L., Dickinson, M., Giavalisco, M., & Pettini, M. 2001, *ApJ*, 562, 95
- Shapley, A. E., Steidel, C. C., Erb, D. K., Reddy, N. A., Adelberger, K. L., Pettini, M., Barmby, P., & Huang, J. 2005, *ApJ*, 626, 698
- Smail, I., Ivison, R. J., Blain, A. W., & Kneib, J.-P. 2002, *MNRAS*, 331, 495
- Somerville, R. S. & Primack, J. R. 1999, *MNRAS*, 310, 1087
- Somerville, R. S., Primack, J. R., & Faber, S. M. 2001, *MNRAS*, 320, 504
- Spergel, D. N. et al. 2003, *ApJS*, 148, 175
- . 2007, *ApJS*, 170, 377
- Springel, V., White, S. D. M., Tormen, G., & Kauffmann, G. 2001a, *MNRAS*, 328, 726
- Springel, V., Yoshida, N., & White, S. D. M. 2001b, *New Astronomy*, 6, 79
- Springel, V. et al. 2005, *Nature*, 435, 629
- Steidel, C. C., Adelberger, K. L., Giavalisco, M., Dickinson, M., & Pettini, M. 1999, *ApJ*, 519, 1
- Steidel, C. C., Adelberger, K. L., Shapley, A. E., Pettini, M., Dickinson, M., & Giavalisco, M. 2003, *ApJ*, 592, 728
- Steidel, C. C., Shapley, A. E., Pettini, M., Adelberger, K. L., Erb, D. K., Reddy, N. A., & Hunt, M. P. 2004, *ApJ*, 604, 534
- Tasitsiomi, A., Kravtsov, A. V., Wechsler, R. H., & Primack, J. R. 2004, *ApJ*, 614, 533
- Tinker, J. L., Norberg, P., Weinberg, D. H., & Warren, M. S. 2007, *ApJ*, 659, 877
- Tinker, J. L., Weinberg, D. H., & Warren, M. S. 2006, *ApJ*, 647, 737
- Tinker, J. L., Weinberg, D. H., Zheng, Z., & Zehavi, I. 2005, *ApJ*, 631, 41
- Vale, A. & Ostriker, J. P. 2004, *MNRAS*, 353, 189
- . 2006, *MNRAS*, 371, 1173
- van den Bosch, F. C. et al. 2007, *MNRAS*, 376, 841
- van Dokkum, P. G. o. 2006, *ApJ*, 638, L59
- Wang, L., Li, C., Kauffmann, G., & de Lucia, G. 2006, *MNRAS*, 371, 537
- Wechsler, R. H., Bullock, J. S., Primack, J. R., Kravtsov, A. V., & Dekel, A. 2002, *ApJ*, 568, 52
- Wechsler, R. H., Gross, M. A. K., Primack, J. R., Blumenthal, G. R., & Dekel, A. 1998, *ApJ*, 506, 19
- Wechsler, R. H., Somerville, R. S., Bullock, J. S., Kolatt, T. S., Primack, J. R., Blumenthal, G. R., & Dekel, A. 2001, *ApJ*, 554, 85
- Weinberg, D. H., Colombi, S., Davé, R., & Katz, N. 2006, *astro-ph/0604393*
- White, M., Zheng, Z., Brown, M. J. I., Dey, A., & Jannuzi, B. T. 2007, *ApJ*, 655, L69
- White, S. D. M. & Frenk, C. S. 1991, *ApJ*, 379, 52
- White, S. D. M. & Rees, M. J. 1978, *MNRAS*, 183, 341
- Willmer, C. N. A. et al. 2006, *ApJ*, 647, 853
- Yan, R., Madgwick, D. S., & White, M. 2003, *ApJ*, 598, 848
- Zehavi, I. et al. 2005, *ApJ*, 630, 1
- Zheng, Z. 2004, *ApJ*, 610, 61
- Zheng, Z., Coil, A. L., & Zehavi, I. 2007, *ApJ*, 667, 760
- Zheng, Z. et al. 2005, *ApJ*, 633, 791
- Zoccali, M. et al. 2003, *A&A*, 399, 931